Universidade Federal de Campina Grande
Brasil

Singular effects on the Hall conductivity

Armelle POUX

Contents

Abstract

Condensed Matter physics is a branch of Physics which includes the laws of quantum mechanics, electromagnetism and statistical mechanics. In this area, we consider a two-dimensional electron gas (2DEG), which can be defined as a system of electrons that are confined by opposing forces to a thin planar region.

Nowadays, it is more interesting to study the impact of the geometry or of some topological defects introduced on the sample, to get closer of reality.

In the work that we have proposed to realize, we have considered a sample immersed on a magnetic field. Or more simply, we wanted to study the Hall effect for particular cases, on usual semiconductors. In fact, we have tried to understand how we can influence the behavior of the Hall conductivity, with a curved surface (rather than the flat case) and by introducing some topological defects.

In a first work, we have considered the single cone immersed into a magnetic field. We realized that we can consider the conical tip in two different ways : with and without a singularity at the tip. We saw that we obtained different Landau Levels LL, which change the type of plateaus that we obtain and the shifting in the Hall conductivity. After discussing this, we changed some parameters (the opening angle α of the cone, the geometric potential) to see how this influenced the Hall conductivity when we varied the magnetic field. We compared two types of geometric models : the da Costa and the Dirac models.

In a second work, we have studied the effect of a screw dislocation on the Hall conductivity. For that, we have changed the torsion parameter of the medium β. We did not observe any shift of the Hall conductivity, but we noticed a change of the size of the conduction plateaus. In order to appreciate the presence of both a screw dislocation and a disclination, we have considered a 2DEG with a dispiration. By changing α, which is the deficit/excess angle, we obtained, this time, a shift of the Hall conductivity.

In summary, we tried to explain the behaviour of the Hall conductivity in the presence of singularities and how taking into account the geometry is important.

Key words : 2DEG, Landau Levels, Hall Conductivity, defects

Acknowledgments

As a prelude to this internship report, I wanted to extend my sincere thanks to persons who gave me their support and contributed to the preparation of this report.

I would like first to sincerely thank Pr. Dr. Cleverson Filgueiras, who as internship supervisor for the theoretical part, was always attentive and very helpful throughout the realization of this internship, as well as for inspiration, help and time he willingly gave me. My thanks also go to Pr. Dr. Lincoln Araujo, internship supervisor for the experimental part, for opening the doors of the experimental laboratory of the university of Campina Grande (and the group of work Rodrigo Lima, Sergio Batista and Kennedy Leite) and to have allowed me to visit the experimental laboratory of Natal (UFRN). And the Pr. Dr. Fernando Moraes (UFPB) and Pr. Dr. Adriano Batista (UFCG) to accept to be my examiners.

Secondly, I would like to thank Ms. Valerie Besombes, Educational Secretary of the University Paul Sabatier, Toulouse, for the kindness and patience she showed during my two years of Master degree, and the University of Toulouse and Midi-Pyrénées region for the financial support they gave me.

I express my gratitude to all persons thanks whom I been able to come to do my internship in Brazil (Pr. Dr. Francisco Brito, Pr. Dr. Michel François Fossy, Pr. Dr. Lucilene Bandeira, Goulwenn Tristant), and all those thanks whom I could discover and "survive" in Brazil (Elizangela Nascimento, Anahi Castro, etc.). I also thank my Portuguese teachers Francinaldo De Souza Lima and Hortência Morais for the patience they have shown in teaching me this language.

I want to especially thank Damient Tristant, who accompanied me on this adventure, with whom I shared all the good and bad moments.

I do not forget my parents, my brother and sister for their encouragement throughout my studies.

Thank you to all of them and the others that I have forgot.

Introduction

Condensed Matter physics finds its starting point in the solid-state theory. In fact, we observed that some theories and concepts could be extended to the study of fluids. Indeed, the properties of a quantum fluid constituted by the conduction electrons in a metal is very similar to those of a fluid made up of atoms, like the strong similarity between conventional superconductivity and superfluidity in helium-3.
In this research area, we consider the system of a two-dimensional electron gas (2DEG), which has become an important branch of science [1]. We can simply define this kind of system as a system of electrons that are confined by opposing forces to a thin planar region adjacent to an interface or within a thin layer of material. But this electrons are free to move along the plane scattering off each other. The scale of this research is limited to micro-macroscopic, which can be studied in the laboratory.

We said that these electrons are free to move. This is true until we introduce an external parameter (for example a magnetic field) causing physical effects such as: Kondo effect, plasmon, quantum Hall effect, Wigner crystal, strongly correlated electrons, photoluminescence, etc. All of those effects permit us to realize the study of our sample and if possible, make new discoveries to improve the already existing technologies. We can also introduce defects, which can be defined as an imperfection in a periodic crystal structure. We can encounter different kinds of defects. The point defects, which occur only at or around a single lattice point (such as vacancy defects, interstitial defects and impurities), the line defects (dislocations, disclinations), the planar defects (grain boundaries, antiphase boundaries), and to finish, the bulk defects.

In our case, we focused our attention in the quantum Hall effect on usual semiconductors. But we will not consider a common semiconductor. Indeed, we wanted to combine the quantum Hall effect with curvature effects. The curvature effects just means that we do not find ourselves in the simplest case that we know, which is the flat case, but in a more complex geometry, such as spherical, cylindrical or conical [2, 3, 4, 5]. Over the last years, technological advances have made possible the investigation of non-planar two-dimensional electron gas (NP2DEG) [4, 6, 7, 8]. Bilayer graphene sheets are candidates in order to explore phenomena induced by geometry in NP2DEG [9]. The Hall conductivity (or resistance) is topologically stable, but the curvature can change the plateau widths and shift the steps in the Hall conductivity [4]. This induces novel phenomena which might be important to engineering quantum devices [9].

The second interesting thought would be the investigation on how topology can influence all types of quantum Hall effect. Since this is not a simple task, we think that we must consider also usual semiconductors. Some ingredients are necessary: first, we must know how conducting electrons on tridimensional solids are studied (this is achieved by the Geometric Theory of Defects [10]); then, we have to obtain the Landau levels LL in a background space with a specific topology (disclination [11], screw dislocation [12], etc...); at the end, we must investigate how these LL are affected by singularities[13]. This theoretical investigation started in [14] where the influence of a topological defects called disclination, on the IQHE was addressed following this recipe.

A fundamental problem that has been discussed in [15] is how the conical tip affects the quantum dynamics on a cone. From a mathematical point of view, there might exist a coupling between the wave functions and the singular scalar curvature on a cone [16]. However, we think that such a coupling should be investigated in an experimental point of view. Because of this view, in this work we obtain the Landau levels on a cone and compare both cases, with and without the singular effect.
For this, we will study the cone with and without singularity at the tip, which are very close cases, but do not necessarily behave the same way. These two different studies appear to us very pertinent, because they could allow us, later, to make progress in the investigation of a graphene sheet.

We will begin our study with theoretical explanations laying down the foundations we need later. So, we will describe the history of the Hall effect (classical and quantum). After that, begin our research work. The second chapter is a study of the cone immersed into a magnetic field. But when we began to study this case, we realized that we can consider the cone in two different ways: with and without a singularity at the tip. We saw that we obtained different LL, which change the type of plateaus that we obtain and shift the Hall conductivity. After discussing this, we tried to change some parameters (the opening angle α of the cone and the geometric potential) to see how this influenced the Hall conductivity when we varied the magnetic field. This comparision will be explained first from a mathematical point of view, and then simulated by using the software $Maple16$.
In the third chapter, we will realize the same kind of study, but now it is for a topological defect introduced on a semiconductor. We studied the effect of a screw dislocation on the Hall conductivity. For that, we changed the torsion parameter of the medium β. We did not observe any shift of the Hall conductivity, but we noted a changing of the size of conduction plateaus. In order to appreciate the presence of both a screw dislocation and a disclination, we have considered a 2DEG with a dispiration. By changing α, which is the deficit/excess angle, we obtained, this time, a shift of the Hall conductivity.

In these two works, we will consider a 2DEG with a screw dislocation. We start by considering a tridimensional solid. The electrons are constrained to a thin interface so the quantum Hall effect can manifest itself. We ignore the fractional quantum Hall effect (FQHE) since the Landau quantization is enough to understand

the IQHE. We consider the fundamental state, $T = 0K$. We do not consider the temperature smearing of the steps of the quantized conductivity[4]. As we said above, our contribution can find place only in usual semiconductors, but we think that understanding how topological defects affect the QHE in this class of materials is a first step to explore the influence of topology on the QHE in other types of materials.

The work presented here is still in progress, so further analysis must be done in order to make a connection with experiments.

Chapter 1

Hall Effect

The Hall effect was discovered in 1879 by Edwin Herbert Hall, during his doctoral degree. He tried to answer a question of James Clerk Maxwell, which was : is the resistance affected by the magnetic field ? He could answer this question experimentally, by using a gold leaf. He managed to highlight the presence of a potential difference V_H, or Hall voltage, between the opposite sides of the gold leaf when it is traversed by electric current, and subjected to a perpendicular magnetic field. This is the effect of a magnetic field on a conductive material through which passes an electric current, which carries the name "Hall Effect".

1.1 Some generalities about the classical Hall Effect

Let us consider a metallic sample under the same conditions as the Hall's experiment succinctly described previously. The sample is bi-dimensional, i.e. a sample so thin that electrons are confined in x- and y-directions, for greater sensitivity. It is traversed by a current I, in the x-direction and immersed in an electromagnetic field in z-direction, B_z, Figure 1.1 (a).

For the classical Hall effect, when we have not any magnetic field, i.e. $B = 0T$, the charge carriers (electron-hole) simply move through the sample in a straight line. So the resistivity is null. However, when a magnetic field with a perpendicular component is applied, their paths are curved. So that moving charges accumulate on one face of the material and induce an electric field. This phenomenon, the curvature of the path of the electrons, happens under the influence of the Lorentz force, due to the electromagnetic field. This implies two types of resistivity : longitudinal resistance and transverse resistance. The longitudinal resistance is the measurement of the parallel resistivity to the current, and the transverse resistance, also called Hall resistance (R_H), is the mesurement of the perpendicular resistivity. If we plot, Figure 1.1 (b) this second resistance depending of the magnetic field, we find a linear variation

$$R_H = \frac{B}{en}, \tag{1.1}$$

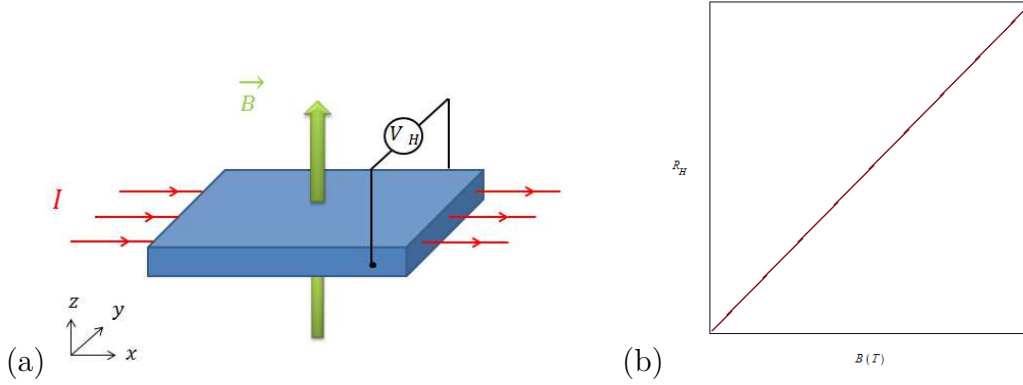where e is the carrier charge and n the 2D carrier density.

Figure 1.1: **(a)** 2D metal traversed by an electric current and subjected to a magnetic field **(b)** Representation of a Hall resistance depending of the magnetic field. We note that we have a linear variation of the Hall resistance when we increase the magnetic field.

One hundred years later, in 1980, Klaus von Klitzing found the Quantum Hall Effect (QHE), or more precisely te Integer Quantum Hall Effect (IQHE).
To show the Quatum Hall Effect, we need to consider a material with a gap energy between the valence band and the conduction band, such as metals or semiconductors. For example the transistors, or Metal-Oxide-Semiconductor Field-Effect Transistors (MOSFET), where the metallic layer is separated from a semiconductor by an insulating oxide layer. He received for this the Nobel Prize in 1985.

1.2 Some generalities about Quantum Hall Effect

The IQHE occurs for a two-dimensional electron system, in the presence of large magnetic field strength and low temperature ($\approx 50mK$), when the energy scale set by the temperature $k_B T$ is significantly smaller than the Landau Level (LL) spacing $\hbar w_C$. We can describe this kind of effect like quantization of the Hall resistance, which is no longer linear in B. Now, the Hall resistance reveals plateaus at particular values of the magnetic field. At each step, these plateaus vary by an integral multiple of h/e^2, where h is Planck's constant. So now, we have, for the Hall resistance

$$R_H = \left(\frac{h}{e^2}\right)\frac{1}{n}, \tag{1.2}$$

where n is a nonzero integer. These plateaus are accompanied by a vanishing longitudinal resistance, as we can see in Fig. 1.2.
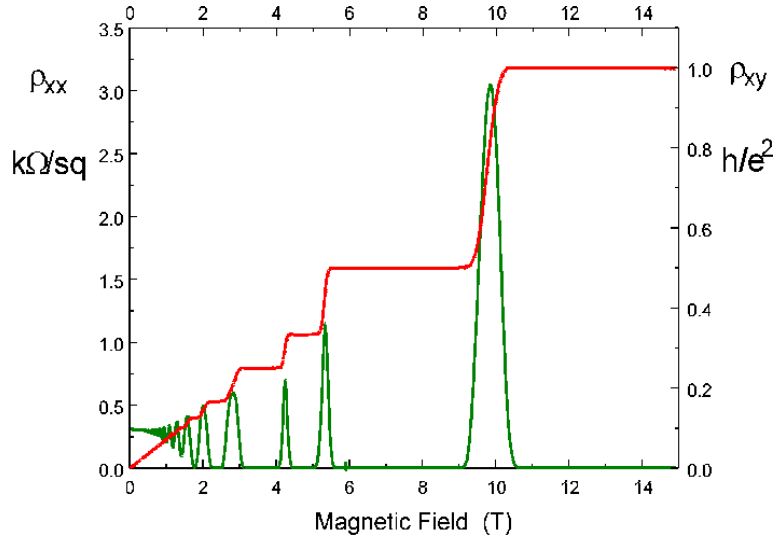
Figure 1.2: The red line is the Hall resistance and the green line the Shubnikov-de Hass oscillations or longitudinal resistance. We observe plateaus of conductivity for the Hall resistance, and for these plateaus, we have the longitudinal resistance which is zero [17].

At low temperatures, in the presence of very intense magnetic fields, the Shubnikov-de Haas effect appears. It is a macroscopic effect which is generated by the intrinsic quantum mechanical nature of matter. In our case, the peaks in the Shubnikov-de Hass oscillations occur at the same magnetic fields as the changes of the plateaus of Hall resistivity. We can explain these occurrences by the fact that when we apply a magnetic field on a 2DEG, the electrons perform a circular motion in the bulk. These electrons perform this movement in a well-defined sense. For example, if there is a negatively charged impurity (-), they rotate in the clockwise direction, and counter-clockwise for a positively charged impurity (+). In the border regions of the sample, the electrons cannot perform full circular motions, so they just follow the edge, moving parallel to the edge of the sample. We can observe this phenomenon in the Fig. 1.3.

These scattering events give to these electrons a higher energy. The eigenvalue energy of the circular motion of these electrons are the same as for the harmonic oscillator with the eigenfrequency ω_C

$$\omega_C = \frac{eB}{m},\tag{1.3}$$

where ω_C is the cyclotron frequency and m the effective mass of the electrons.

In the presence of a magnetic field, if we calculate the energy levels of the 2DEG, we can notice that they are quantized into discrete levels, called Landau levels.
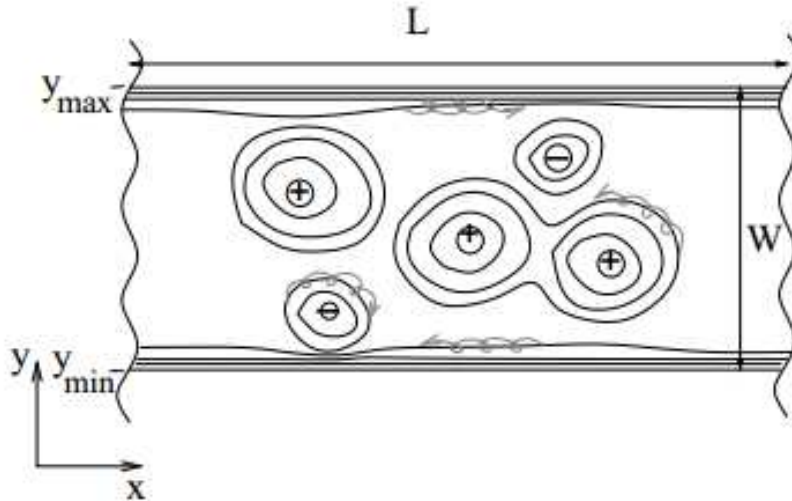
Figure 1.3: Here is a sample whose length L is much larger than the width W, where we will see that the electrons near the edge have a displacement parallel to the edges of the sample and the core electrons a circular motion, whose the direction depends on the sign of the impurities [17].

1.3 Landau quantization

The Landau quantization can be simply explained as the kinetic-energy quantization of a 2D particle in a perpendicular magnetic field. Effectively, in the presence of a magnetic field, the electronic continuum of states that we had in the case of conventional Hall effect is quantified in energy levels or Landau Levels (LL), according to the expression : $E_n = \hbar w_C(n+1/2)$. These levels are eventually split into electronic sublevels spin parallel or antiparallel to the field, due to the Zeeman effect or other mechanisms related to electron-electron interactions and will not be discussed here. Thereby, the more we increase the magnetic field, the more the difference between two adjacent energies grows. In fact, as we have told before, the difference between two LL is $\hbar w_C$, and from Eq. (1.3), we find $\hbar w_C = \hbar \frac{eB}{m}$. Then, the energy gap between two levels depends on the magnetic field. We can conclude, when we observe the Figure 1.4 that the more we increase the magnetic field, the less LL we have below the Fermi-energy level.

So, let us consider a simple case of a particle confined to the xy-plane. We have the Landau gauge $A_L = B(-y, 0, 0)$ and the resulting Hamiltonian for non-relativistic 2D charged particles

$$H = \frac{1}{2m} \left(\mathbf{p} - e\mathbf{A} \right)^2 + V(y), \tag{1.4}$$

with V(y) the confinement potential of the electrons in the sample and $\mathbf{p} = (p_x, p_y, p_z)$ is the momentum which is the constant of motion. If we do not consider the edges states, we consider just the bulk, we have $V(y) = 0$, so simply
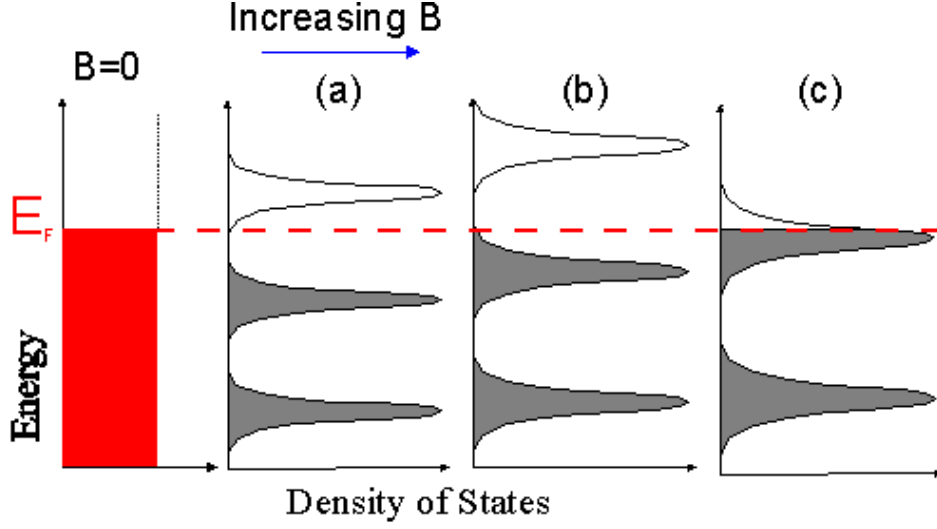
Figure 1.4: Evolution of the Landau Levels when we increase the magnetic field. We can see that the more we increase the magnetic field B, the less LLs are under the Fermi-energy level [17].

$$H = \frac{1}{2m} \left(\mathbf{p} - e\mathbf{A}\right)^2.$$

(1.5)

The translational invariance along the x-direction means that the wave functions have the following form

$$\psi(x, y) = e^{ikx}\psi(y).$$

(1.6)

We know too that $H\psi(x, y) = E\psi(x, y)$, so

$$E\psi(y) = \left(\frac{P_y^2}{2m} + \frac{1}{2}m\omega_C^2(y - y_c)^2\right)\psi(y),$$

(1.7)

where ω_c is the cyclotron frequency. In the center of the sample, the potential $V(y)$ is zero and the energy levels does not depend of the position y_c, so the energy levels are independent of the position and we find the same case as the harmonic oscillator. We can write

$$E = \hbar w_C \left(n + \frac{1}{2}\right),$$

(1.8)

where n is an integer, the LL number. If we plot few of these levels, we obtain the Fig. 1.5, where we can see that we have the same distance between two consecutive levels.
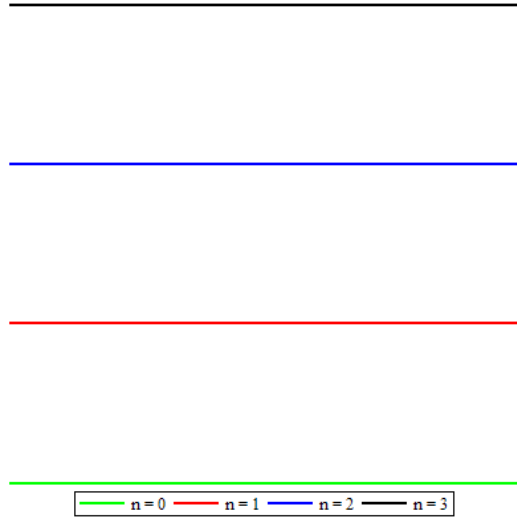
Figure 1.5: LLs for a flat case. This plot indicates that we have a constant energy interval between two adjacent levels.

1.4 Hall conductivity

When we obtain the LL, we can deduce the Hall conductivity dependence on the magnetic field. For example, if we take $n = n_0 - 1$, with $n = 0, 1, 2, ..$ and $n_0 = 1, 2, 3, ..$, we obtain, from the equation (1.8)

$$E = \hbar w_C \left(n_0 - \frac{1}{2} \right). \tag{1.9}$$

When we calculate n_0, in fact, we calculate a starting point for our plateaus, which will the maximum level that we can treat. This maximum corresponds to $B = 10$T here. In this case, we get $n_0 = 17.5$. As n_0 (and n) can only be a nonzero integer, so we take just the integer part of our result. We obtain $n_0 = 17$ which is going to be the highest level we are going to consider. We must have to do this calculation for each particular case.

After we were able to determine our n_0, we can calculate the magnetic field that will be required for each following energy levels. So, we determine the quantity of magnetic field required to move from one state to another, ΔB_n. To determine this value, we simply calculate the numerical value of the magnetic field at each level of energy (by diminishing $n_0 \longrightarrow n_0 - 1$ each time). Finally, we subtract the two by two consecutive levels, and obtain ΔB_n. When we do this calculation, we determine in fact just the size of our plateaus, at zero temperature, in the Hall conductivity, depending on the level changes.

When we have calculated all this, we can then plot the plateaus. In fact, we start at $n_0 = 17$, in our case, and $B = 10T$, and while changing the value of the state n_0 ($n_0 - 1 = n_0$), we add the ΔB_n one by one. When we plot n_0 depending of $B = 10T$, we have $\nu = -\frac{\sigma_H}{\sigma_0}$, where σ_H is the Hall conductivity, $\sigma_0 (= -\frac{e^2}{h})$ is the

quantum of conductivity, and ν is the filling factor.

If we take the simple case, i.e. a flat case, without any effect, any special geometry, or any defects, we obtain the Fig 1.6.
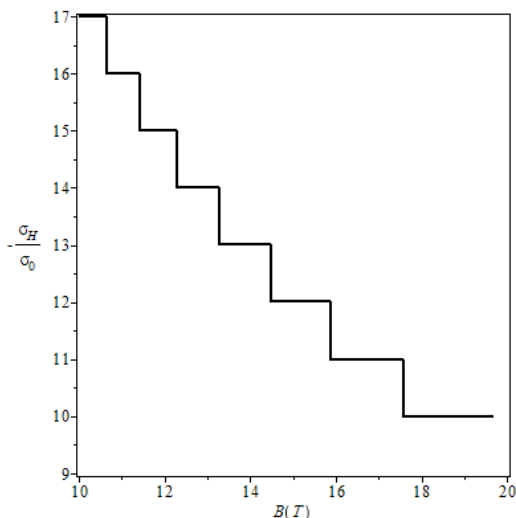

Figure 1.6: Hall conductivity depending of the magnetic field B for a flat case, at $T = 0$K.

The IQHE is not the only known kind of quantum Hall effect. In fact, there is also the Fractional Quantum Hall Effect (FQHE) that was discovered only three years later, by Robert Laughlin, Horst Störmer and Daniel Tsui, in a 2D electron system of higher quality (i.e. higher mobility). The difference with the IQHE it is that instead of having a strictly integer value for the resistance, we have a value with a fractional part, for example $n = 1/3$. The FQHE is due to strong electronic correlations, when a LL is only partially filled and the Coulomb interaction between the electrons becomes relevant. But we will not provide further explanations on this second effect, since it will not be necessary in our study.

Getting back to our graphic (Fig. 1.6), the kind of plateaus that we obtain depends on many parameters. For example, if the energy levels have a lifting of degeneracy, if we introduce some kind of deformations, if we change the geometry, etc. So, for each case that we would like to study, we have to choose good parameters and see what happens if we change them.

In this Chapter, we studied some generalities about the Hall effect, applied to a flat case. In the following Chapters, we will discuss the behavior of the Hall conductivity in the presence of curvature singularities.

Chapter 2

Integer Quantum Hall Effect on a cone

After reviewing all of this, we have all the tools to study the consequences of the Hall effect on a cone. Effectively, we would like to find the consequences for a conical surface when we apply a magnetic field. In the first time, we will study the Hall conductivity for a cone with and without singularity at the tip. Then, to go further in this study, we will change some parameters in our calculations.

In all our investigation we have characterized only the IQHE because if we consider the FQHE, like we have explained in section 1.4, we have to take into account the Coulomb interaction, and the problem becomes more difficult. Moreover, this was not the aim of our study.

2.1 Schrödinger equation and Landau Levels

Let us consider the coordinates of a particle confined to the surface of a cone as

$$\begin{cases} x = l \sin\alpha \cos\varphi \\ y = l \sin\alpha \sin\varphi \\ z = l \cos\alpha \end{cases} , \tag{2.1}$$

where $0 \leq \varphi \leq 2\pi$, $0 \leq \alpha \leq \pi$ and $0 < l < +\infty$.

Consider an applied magnetic field in the $z-$direction, $\vec{B} = (0, 0, B_z)$. By using the Stokes theorem, we can calculate the vector potential $\vec{A}$. Considering the equation

$$\vec{B} = \vec{\nabla} \times \vec{A} , \tag{2.2}$$

we have

$$\int_S \vec{B} \cdot d\vec{S} \equiv \int_S \vec{\nabla} \times \vec{A} \cdot \hat{n} dS = \oint_{\partial L} \vec{A} \cdot d\vec{L} , \tag{2.3}$$

where S is a surface in Euclidean three-space, ∂L is its boundary and $\hat{n}$ is the normal unit vector to the surface. For a cone, we have
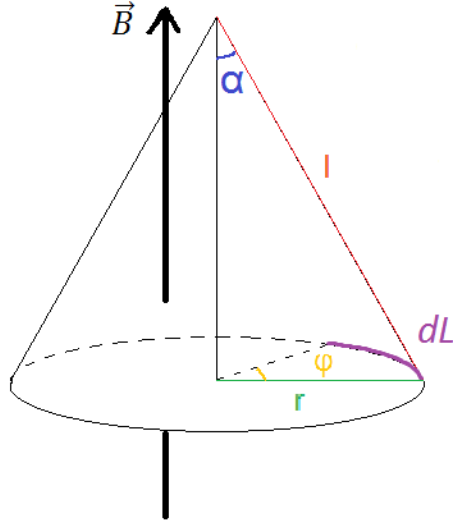
$$dS = \sin\alpha \, l dl d\varphi \tag{2.4}$$

Figure 2.1: A cone immersed in a magnetic field in the z-direction.

and

$$dL = \sin \alpha l d\varphi .$$

(2.5)

Then,

$$\int B_z \hat{z} \cdot \hat{n} \sin \alpha l dl d\varphi = \oint_{\partial L} \vec{A} \cdot \sin \alpha l \vec{d\varphi}$$

(2.6)

Choosing $\vec{A}(l, \varphi, z) = (0, A_\varphi, 0)$, it yields

$$\sin^2 \alpha \int B_z l dl d\varphi = \sin \alpha \oint_{\partial L} A_\varphi l d\varphi$$

(2.7)

where we have considered $\hat{z} \cdot \hat{n} = \sin \alpha$. Then,

$$A_\varphi = \frac{B_z l}{2} \sin \alpha .$$

(2.8)

We can now write the Schrödinger equation for a charged particle confined to the surface of a cone immersed in an external magnetic field in the $z-$direction. From (2.1), the map of a cone is $\vec{X}(l, \varphi) = (l \sin \alpha \cos \varphi, l \sin \alpha \sin \varphi, l \cos \alpha)$. The coefficients of the induced metric are given by [18]

$$g_{11} = X_l \cdot X_l = \frac{\partial \vec{X}}{\partial l} \cdot \frac{\partial \vec{X}}{\partial l} = 1 ,$$

(2.9)

$$g_{12} = X_l \cdot X_\varphi = \frac{\partial \vec{X}}{\partial l} \cdot \frac{\partial \vec{X}}{\partial \varphi} = 0 ,$$

(2.10)

$$g_{22} = X_\varphi \cdot X_\varphi = \frac{\partial \vec{X}}{\partial \varphi} \cdot \frac{\partial \vec{X}}{\partial \varphi} = l^2 \sin^2 \alpha .$$

(2.11)

So, the metric tensor and its inverse are

$$g_{ij} = \begin{pmatrix} 1 & 0 \\ 0 & l^2 \sin^2(\alpha) \end{pmatrix}$$

(2.12)

16

and

$$g^{ij} = \begin{pmatrix} 1 & 0 \\ 0 & \frac{1}{l^2 \sin^2(\alpha)} \end{pmatrix} , \qquad (2.13)$$

respectively. We consider the Hamiltonian for a charged particle as

$$\hat{H} = \frac{1}{2m} (\hat{p} - e\hat{A})^2 . \qquad (2.14)$$

In order to ensure the hermiticity of radial momentum operator, $\hat{p}_l$, it must act on the radial wave functions as

$$\hat{p}_l \psi(l) = -i\hbar \left(\frac{\partial}{\partial l} + \frac{1}{2l} \right) \psi(l). \qquad (2.15)$$

We refer the reader to reference [19] to go into the details of this last relation. So, we achieve

$$\hat{H} = -\frac{\hbar^2}{2m} \left[\frac{1}{l} \frac{\partial}{\partial_l} \left(l \frac{\partial}{\partial_l} \right) - \frac{1}{4l^2} - \left(-\frac{i}{l \sin \alpha} \frac{\partial}{\partial_\varphi} - \frac{e \sin \alpha B_z l}{2\hbar} \right)^2 \right] \qquad (2.16)$$

for the Hamiltonian for the particule moving on the cone. We have used $p_l^2 = -\hbar^2 \nabla_l^2$, with $\nabla_l^2 \equiv \frac{1}{\sqrt{g}} \partial_l \sqrt{g} g^{11} \partial_l$, $g = \det(g_{ij}) = l^2 \sin^2 \alpha$ and $p_\varphi = -\frac{i\hbar}{l \sin \alpha} \partial_\varphi$. It is important to notice that the Schrödinger equation for a quantum particle on curved surfaces exhibits a scalar potential which describes the interaction of quantum particles with geometry. It was shown in [20] that this potential does not couple with the magnetic field. It is given by

$$V_S = -\frac{\hbar^2}{2m} \left(M^2 - K \right) = -\frac{\hbar^2}{2m} \left(k_1 - k_2 \right)^2 . \qquad (2.17)$$

In these expressions, k_1 and k_2 are the principal curvatures, $M \equiv \frac{1}{2}(k_1 + k_2)$ is the mean curvature and $K \equiv k_1 k_2$ is the Gaussian curvature of a given surface [18]. This potential was first derived in [21]. This way, the Schrödinger equation is $\left[\hat{H} + V_S \right] \Psi(l, \varphi) = E\Psi(l, \varphi)$. So, we have

$$-\frac{\hbar^2}{2m} \left[\frac{1}{l} \frac{\partial}{\partial l} \left(l \frac{\partial}{\partial l} \right) - \frac{1}{4l^2} - \left(\frac{-i}{l \sin \alpha} \frac{\partial}{\partial_\varphi} - \frac{e \sin \alpha B_z l}{2\hbar} \right)^2 \right] \Psi(l, \varphi) + V_S \Psi(l, \varphi) = E\Psi(l, \varphi) . \qquad (2.18)$$

We may calculate M and K by the formula [18]

$$M = \frac{1}{2} \frac{eG - 2fE + gE}{EG - F^2} \qquad (2.19)$$

and

$$K = \frac{1}{2} \frac{eg - f^2}{EG - F^2} , \qquad (2.20)$$

respectively. For a cone, $E = g_{11} = 1$, $F = g_{12} = 0$, $G = g_{22} = l^2 \sin^2 \alpha$, $e = \vec{n} \cdot \frac{\partial^2 \vec{X}}{\partial \varphi^2} = 0$, $f = \vec{n} \cdot \frac{\partial^2 \vec{X}}{\partial \varphi \partial l} = 0$ and $g = \vec{n} \cdot \frac{\partial^2 \vec{X}}{\partial l^2} = l \sin \alpha \cos \alpha$. This way, $M = \frac{\cos \alpha}{2 \sin \alpha l}$ and $K = 0$.

By considering the wave function as $\Psi(l, \varphi) = \Psi(l) e^{ij\varphi}$, with $j = 0, \pm 1, \pm 2, ...$, we arrive at

$$-\frac{\hbar^2}{2m} \left[\frac{1}{l} \frac{d}{dl} \left(l \frac{d}{dl} \right) - \frac{\frac{1}{4} + \frac{\mu^2}{\sin^2 \alpha}}{l^2} \right] \Psi(l) + \frac{mw^2 l^2}{2} \Psi(l) = \Sigma \Psi(l) \qquad (2.21)$$

where $\mu^2 = j^2 - \frac{1 - \sin^2 \alpha}{4}$, $\omega = (\omega_c/2) \sin \alpha$, with $\omega_c = \frac{eB_z}{m}$ the cyclotron frequency, and

$$\Sigma = E + j\hbar\omega . \qquad (2.22)$$

This differential equation describes a two dimensional quantum oscillator on a conical background. This problem was addressed in [22] for a circular double cone. Since we get the same differential equation found in [22], the wave functions are generally given by

$$\Psi(l) = \mathrm{C} \, |l|^s \exp(-\frac{m\omega^2 l^2}{2}) U \left(\frac{s}{2} + \frac{1}{4} - \frac{E}{2\omega}, s + \frac{1}{2}, m\omega l^2 \right) \qquad (2.23)$$

with

$$s = \frac{1}{2} \left(1 \pm \sqrt{1 + \frac{4\mu^2}{\sin^2 \alpha}} \right) \qquad (2.24)$$

and C being the normalization constant. $U(a, b, c)$ is the Kummer function [23], see Appendix D.

In the case of 2DEG on a cone, the range of the coordinate l is $0 < l < +\infty$, whereas that for a circular double cone it is $-\infty < l < +\infty$. In order to have normalization of the wave function, we have

$$\lim_{l \to \infty} \Psi(l) \longrightarrow 0. \qquad (2.25)$$

If we consider the equations on the Appendix D, and

$$\int_0^\infty |\psi|^2 \, l dl < \infty, \qquad (2.26)$$

we get

$$\int_0^\infty |\psi|^2 \, l dl = A l'^{2s+2}, \qquad (2.27)$$

where A is a constant.

Before doing any further analyses, we must mention that, as it was argued in Refs. [15, 22], that the tip of the cone corresponds to a singularity and the quantum dynamics requests self-adjoint extensions [24, 25], in contrast with the double cone case, where such singular effects can not show up. Notice that the case of quantum particles around a double cone is similar to the one where we have quantum particles on a cone without the coupling between the wave functions and a singular curvature. This is a situation without δ-function potentials, which correspond the so-called Friedrichs extension [24]. It is characterized by the following boundary condition,

$$\lim_{l \to 0} l \partial_l \psi(l) = 0. \qquad (2.28)$$

This condition means that, although we have a conical tip, the wave functions are regular at $l = 0$. When we consider the $\delta-$function potential, the quantum dynamics

request self-adjoint extensions since the wave functions now are irregular at $l \to 0$ [26]. In what follows, we evoke the results of [22] for the regular case and after that we discuss what is going to change when we take into account the wave functions being irregular at the conical tip.

For electrons on a cone without the coupling with the singular Gaussian curvature, the parameter s above must be just that with a plus sign. Notice that, for positive s, (2.26) goes to zero as $l \longrightarrow 0$. Since we do not have singularity, this means that the wave functions are regular at the conical tip. So, the eigenvalues are given by

$$\Sigma_{j,n} = 2\hbar\omega \left(n + \frac{1}{2} + \frac{1}{4}\sqrt{1 + \frac{4\mu^2}{\sin^2\alpha}} \right). \tag{2.29}$$

Combining this equation with (2.32), we arrive at the Landau levels for electrons on a cone, that is,

$$E_{j,n} = \hbar\omega_c \sin\alpha \left(n + \frac{1}{2} + \frac{1}{4}\sqrt{1 + \frac{4\mu^2}{\sin^2\alpha}} - \frac{j}{2} \right). \tag{2.30}$$

The problem addressed here has an important difference from that investigated in [22]. First of all, Eq. (2.30) has an extra piece proportional to $-\frac{j}{2}$. Also, the term inside the square root in Eq. (2.30) shows the parameter μ^2 (instead of just j^2) which can never be null for integer values of j. If we take $j = 0$ in equation (2.21) we get the same result as taking $j \to 0$ in (2.30), in contrast with [22], where the results are different. This solution corresponds to the case of a harmonic oscillator on a meridian of the cone. This difference comes from the interaction with the geometric potential V_S which leads to an inverse square distance dependent quantum potential.

We now turn our attention to the case where there is the coupling between the wave functions and the singular Gaussian curvature. The problem concerning the quantum harmonic oscillator with singularities was addressed in Ref. [26]. Everything we have done so far remains the same but in order to have irregular wave functions as $l \to 0$ that are still square integrable, the parameter s (2.24) now admit both signs, plus and minus. The case with minus sign correspond to wave solutions which are irregular at the tip of the cone. In order to have

$$\int_0^\infty |\psi|^2 \, l\,dl = A l^{2s+2} \longrightarrow 0, \tag{2.31}$$

we must impose the constrain

$$-1 < s < 1 \,, \tag{2.32}$$

to guarantee that the wave functions are square integrable. Whenever we have singularity, this conditions must happen [27]. In order to fulfill (2.32), the only possible value for the angular momentum is $j = 0$. Then, the Landau Levels split as

$$E_{0,n}^+ = \hbar\omega_c \sin\alpha \left(n + \frac{1}{2} + \frac{1}{4}\sqrt{2 - \frac{1}{\sin^2\alpha}} \right) \tag{2.33}$$

and

$$E_{0,n}^{-} = \hbar\omega_c \sin\alpha \left(n + \frac{1}{2} - \frac{1}{4}\sqrt{2 - \frac{1}{\sin^2\alpha}} \right) . \tag{2.34}$$

In summary, without singular effects, the Landau levels are those obtained as (2.30), with $j = 0, \pm 1, \pm 2, ...$ If the singular Gaussian curvature plays a role, than the only possibility will be $j = 0$. In the former case, the degeneracy is infinitely broken in comparison to the flat case ($j = 0, \pm 1, \pm 2, ...$) and in the latter one, each Landau level is splitted twice. We sketch the Landau levels for both problems in figure 2.2.

In this section we addressed the Landau levels for a 2DEG on both regular and irregular cases. We have seen some fundamental differences which could be detected in a Hall measurement. So, we discuss the quantum Hall effect in what follows.
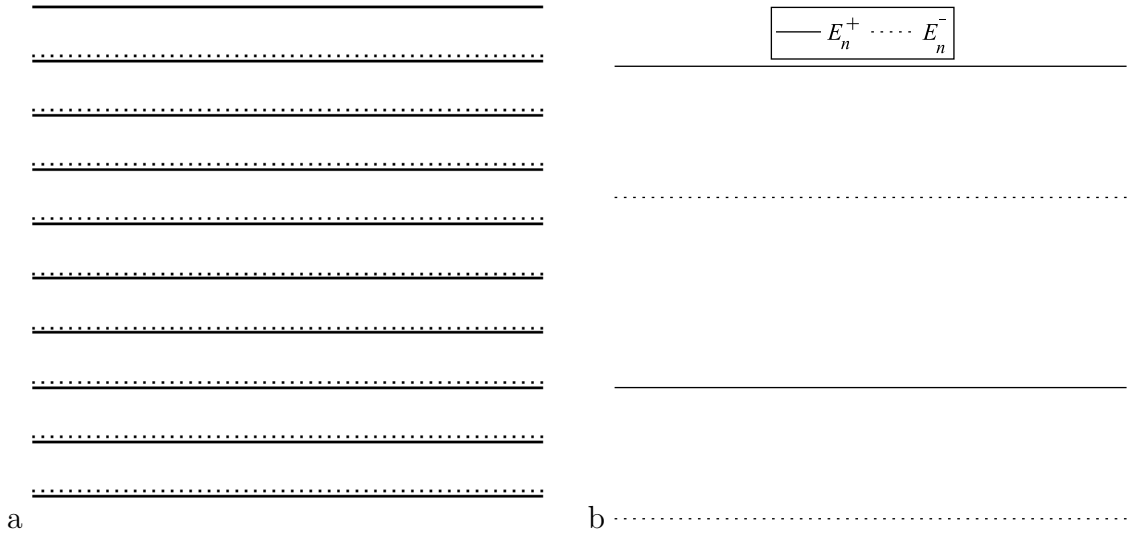

Figure 2.2: (**a**) Some Landau levels for a 2DEG on a cone without singular effects and (**b**) with singular effects(we considered just three filled angular momentum states, $j = -1, 0, 1$). In both cases, $\alpha = \pi/3$ rad.

2.2 Hall conductivity

In this section, we compute the Hall conductivity of a 2DEG on a cone. We consider just the integer quantum Hall effect, which consists of a quantization of the conductivity and appearance of plateaus at particular values of the external magnetic field. It manifests at low temperatures. We take into account just the fundamental state, $T = 0$. Each Landau level contributes one quantum of conductivity to the electronic transport. If n_0 Landau levels are completely filled, the Hall conductivity, σ_H, will be given by

$$\sigma_H = -n_0 \sigma_o , \tag{2.35}$$

where $\sigma_o \equiv e^2/h$ is the quantum of conductivity, e is the electron charge and h is the Planck's constant. The Hall conductivity is independent of a particular sample geometry[28] but a particular geometry like a cone changes the position of the plateaus and their widths. This is what we are going to see bellow.

We start the calculations determining n_0 for a specific value of magnetic field. This is achieved by counting how many states are occupied bellow the Fermi energy, E_F. We compare E_F with the Landau levels showed in figures 3.1, making it equal to the highest Landau level filled. Next, we determine the quantity of magnetic field required to move the Hall conductivity from $-n_0\sigma_o$ to $-(n_o - 1)\sigma_o$. In doing that, we are, in fact, determining the size of the plateaus at zero temperature for a specific n_o. Continuing this procedure, we can then plot the Hall conductivity versus the plateaus. In our calculations, we start at $B = 10T$.
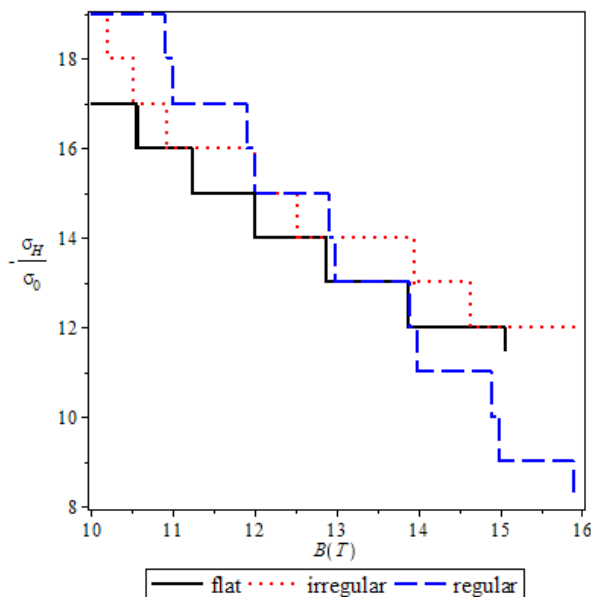

Figure 2.3: Hall conductivity in flat space (full line) and on the cone: with singularity (dot line) and without singularity (dash line). We see that the plateaus of conductivity on the cone are shifted to higher magnetic fields in both cases. We can see clearly that the singular boundary conditions change significantly the Hall conductivity profile. We considered $\alpha = \frac{\pi}{3}$rad.

In figure 2.3 we plot the Hall conductivity for three different cases: a flat sample without singularity and the cone with and without singularity. In the last case we considered just the filled states $j = -1, 0, 1$ only. We can observe that we have intermediate plateaus in this case in comparison to the Hall conductivity on a cone with singularity. If we take more values of j, which is not allowed for the Landau levels in the singularity case, we will obtain other intermediate plateaus. Notice that the plateaus are smaller if we take the cone with singularity in comparison with the flat case. This difference is even more apparent if we compare the flat case with a cone without singularity.

2.3   Impact of the angle α on Hall conductivity of the double cone

In figure 2.4, we probe the influence of the opening angle α. We compare with the flat case. We see that we have the same kind of shifting for both cases, i.e., when we have a little opening angle $\left(\frac{\pi}{4}\right)$, the plateaus are shifted to higher magnetic fields and when we have a big opening angle $\left(\frac{2\pi}{5}\right)$, the plateaus are shifted to smaller magnetic fields. We can also observe that, for a big opening angle, we approach to the flat case. With these plots, we can more easily see that we have a reduction of the size of the plateaus in comparison to the flat case. In analyzing both figures 2.3 and 2.4, we observe that considering or not the singular effects on the wave functions is an important issue on a theoretical basis. We hope this fact will eventually be probed in an experimental point of view.
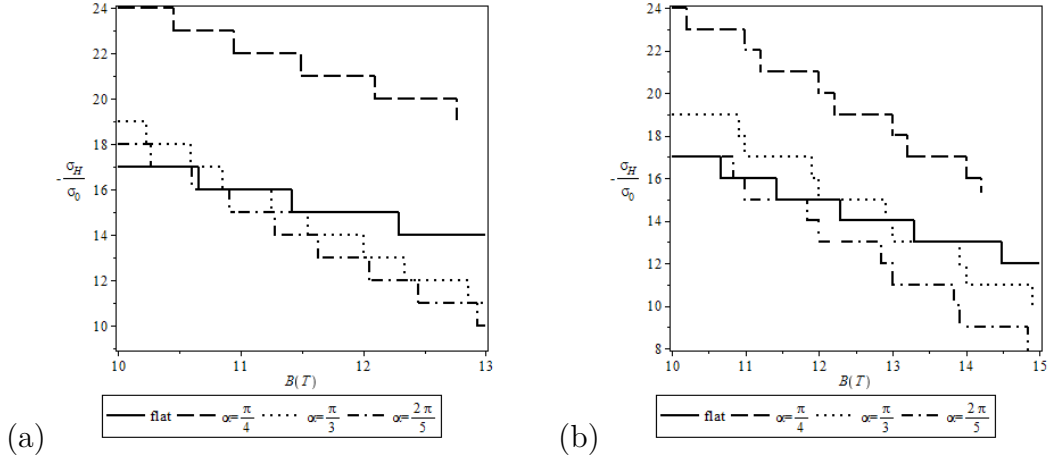

(a)   (b)

Figure 2.4: Hall conductivity on the cone for different opening angles. **(a)** with singular effects and **(b)** no singular effects. Notice again that considering or not the singularity in the wave functions has important consequences.

2.4   Impact of the geometric potential H for the double cone

We now move to see the influence of the mean curvature, that is, we probe the two models we are dealing with for electrons on a curved surface. We consider both cases, with and without singular effects. In the figure 2.5, we can see that, depending on the opening angle α, the two models may yield or not different quantitative results. Indeed, for the singular case and for $\alpha = \frac{\pi}{3}$, the plateaus are shifted to lower magnetic fields. This happens because of the size of the plateaus, which are smaller when we consider the mean curvature potential. For $\alpha = \frac{2\pi}{5}$, taking or not into account the mean curvature potential does not make any difference. Without singular effects, the same thing happens. The difference is only that pointed out in figures 2.3 and 2.4.
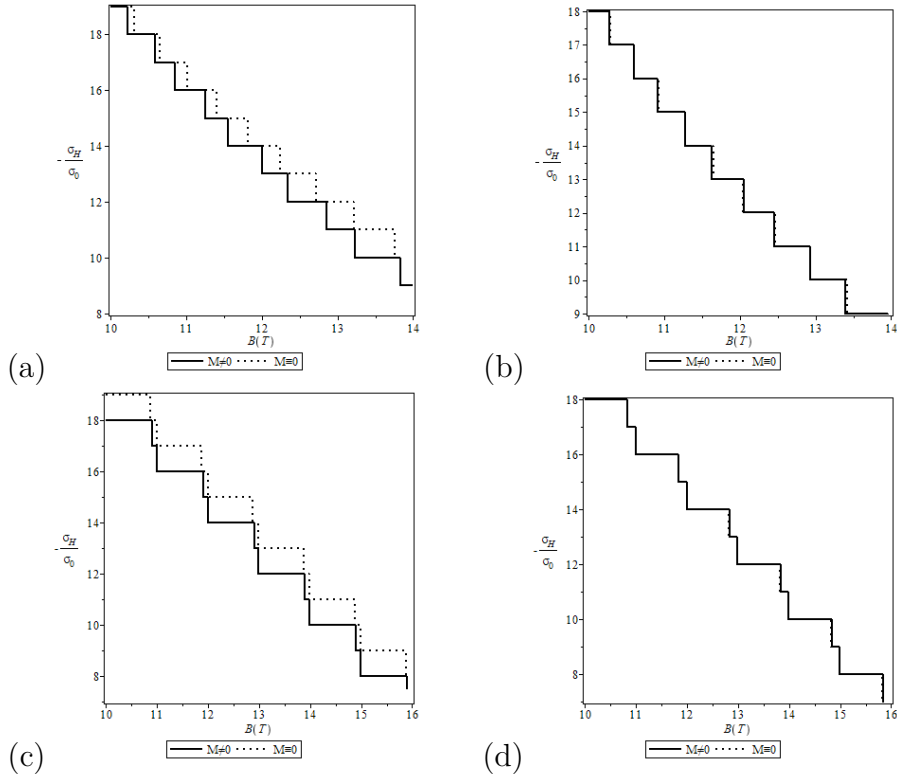
Figure 2.5: Hall conductivity on the cone with and without the mean curvature potential M: without singularity, we have **(a)** $\alpha = \frac{\pi}{3}$ and **(b)** $\alpha = \frac{2\pi}{5}$, while with singularity we have **(c)** $\alpha = \frac{\pi}{3}$ and **(d)** $\alpha = \frac{2\pi}{5}$. Notice that the difference between both approaches may be noted depending on the opening angle α which is considered(see figure 2.6).

Plotting the mean curvature potential M as a function of the opening angle α, we obtain the figure 2.6. That explains clearly what happens in figure 2.5. Indeed, when we have a big opening angle, we can see that the mean curvature potential goes to zero. This is why we have seen in our plots that when we take a big opening angle, taking or not into account M does not make a big difference, contrary to a small opening angle. This said, we conclude that depending on the opening angle of the cone, the difference between the two approaches discussed here for electrons on curved surfaces will not show up. This fact may happen for other geometries. So, comparing the mean curvature with the Gaussian curvature first can tell us when it is important to take it into account in our calculations.

In this first part of our work, we have seen how the geometry of a given sample can change de Hall conductivity. In the second part, we will study the effect of a screw dislocation on the Hall conductivity of a 2DEG.
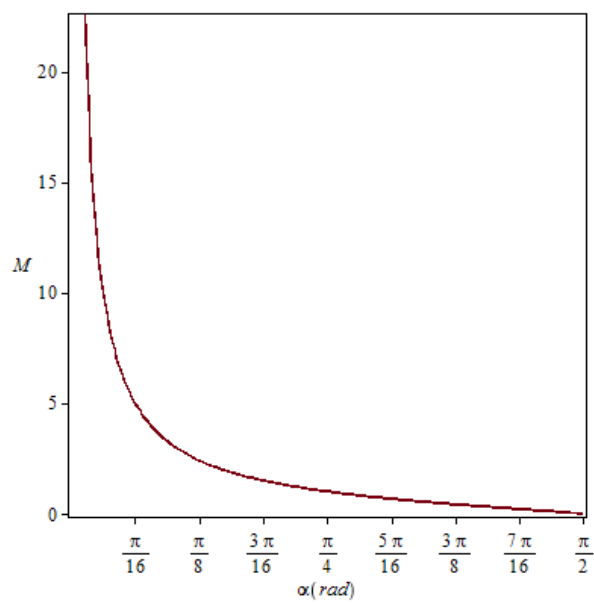
23

Figure 2.6: Profile of the mean curvature M depending on the opening angle α. We can see that, for a smaller values of α, M grows while for higher values of α approaching $\pi/2$, $M \longrightarrow 0$. So, we can see which interval of α the mean curvature contribution to the geometric potential will be relevant.

Chapter 3

Integer Quantum Hall Effect in a medium with a screw dislocation

3.1   Schrödinger equation and Landau Levels

We consider an infinitely long linear screw dislocation oriented along the $z-$axis. The three-dimensional geometry of the medium is characterized by torsion which is identified with the surface density of the Burgers vector in the classical theory of elasticity. The metric of the medium with this kind of defect is given by[10]

$$ds^2 = (dz + \beta d\phi)^2 + d\rho^2 + \rho^2 d\phi^2 \ , \tag{3.1}$$

in cylindrical coordinates. In (3.1), β is a parameter related to the Burgers vector b by $\beta = b/2\pi$. No curvature is induced by this topological defect. Its induced metric describes a flat medium with a singularity at the origin. The only non-zero component of the torsion tensor in this case is given by the two form

$$T^1 = 2\pi\beta\delta^2(\rho)d\rho \wedge d\phi \ , \tag{3.2}$$

with $\delta^2(\rho)$ being the two-dimensional delta function in flat space. We consider a constant magnetic field in the $z-$ direction, $\vec{B} = B\hat{z}$. We choose the vector potential in the background space (3.1) as $A_\phi = \frac{B_z\rho}{2}$[11].

The Schrödinger equation for a free particle in a background $g_{\mu\nu}$ is given by

$$\frac{-\hbar^2}{2m} \frac{1}{\sqrt{g}} \partial_\mu \sqrt{g} g^{\mu\nu} \partial_\nu \Psi = E\Psi \ , \tag{3.3}$$

where $g \equiv \det g_{\mu\nu}$. For electrons in the presence of an external magnetic field, we have $i\partial_\mu \to i\partial_\mu - eA_\mu$. Then, the Schrödinger equation for an electron in a medium with a screw dislocation in a homogeneous magnetic field in the $z-$direction is

$$- \ \frac{\hbar^2}{2m^*} \left[\frac{1}{\rho}\frac{\partial}{\partial\rho}\left(\rho\frac{\partial}{\partial\rho} \right) + \frac{1}{\rho^2}\left(\frac{\partial}{\partial\phi} - \beta\frac{\partial}{\partial z} \right)^2 \right]\Psi +$$

$$+ \ \frac{i\hbar e B_z}{2m^*}\left(\frac{\partial}{\partial\phi} - \beta\frac{\partial}{\partial z} \right)\Psi + \frac{e^2 B_z^2 \rho^2}{8m^*}\Psi -$$

$$- \ \frac{\hbar^2}{2m^*}\frac{\partial^2\Psi}{\partial z^2} = E\Psi \ . \tag{3.4}$$

By considering the wave function as $\Psi(\rho, \phi, z) = e^{i\ell\phi}e^{ik_z z}\psi(\rho)$, with $\ell \in Z$ and $k_z \in \Re$, equation (3.4) yields

$$-\frac{\hbar^2}{2m^*}\left[\frac{1}{\rho}\frac{d}{d\rho}\left(\rho\frac{d}{d\rho}\right) - \frac{\nu^2}{\rho^2}\right]\psi - \frac{\nu\hbar eB_z}{2m^*}\psi +$$
$$+\frac{e^2 B_z^2 \rho^2}{8m^*}\psi = E_{n,\ell}\psi \, , \qquad (3.5)$$

where $E_{n,\ell} = E - \frac{\hbar^2 k_z^2}{2m^*}$ and $\nu = \ell - \beta k_z$. This equation describes the two-dimensional quantum harmonic oscillator in the presence of a screw dislocation.

Let us point out that the eq. (3.5) looks like the same as in the case of a disclination [14]. The only difference is that in the case of a screw dislocation the parameter ν is related to the Burgers vector while in the case of a disclination it is related to the deficit/excess angle α characterizing the defect($\nu = l/\alpha$). So, the two problems can be treated on completely equal footing. However, while a disclination is related to lattice rotations, a dislocation is related to lattice translations and the influence on the Hall effect will be different.

The energy eigenvalues are

$$E_{n,\ell} = \hbar\omega_c\left(n + \frac{|\nu| - \nu}{2} + \frac{1}{2}\right) \, , \qquad (3.6)$$

where $n = 0, 1, 2, ...$ and $\ell = 0, \pm 1, \pm 2, ...$ The respective wave functions, by using the same method of the first chapter, which will give us the effect of a screw dislocation on the Hall conductivity of a 2DEG are

$$\psi(\rho) = C \exp\left(-\frac{m\omega_c}{4\hbar}\rho^2\right)\rho^\nu U\left(-n, \nu + 1, \frac{m\omega_c}{2\hbar}\rho^2\right) \, , \qquad (3.7)$$

where C is a normalization constant.

As we have said above, the screw dislocation induces a singularity in the medium. This means that the electrons are moving in a sample showing singularity. The investigation of quantum systems in this scenario has been carried out over the years [29]. In reference [13], the harmonic oscillator in spaces with singularities was addressed and the effect of such singularities is to restrict the range of allowed values for the effective angular momentum ν, that is,

$$-1 < \nu < 1 \, . \qquad (3.8)$$

This relation holds in order to satisfy the square-integrable condition of wave functions, that is,

$$\int_0^\infty |\psi|^2 \rho d\rho < \infty \, .$$

Notice that the degeneracy of the LL is broken due to the torsion parameter β. In fact, if $\beta \equiv 0$,

$$E_{n,\ell} = \hbar\omega_c\left(n + \frac{|\ell| - \ell}{2} + \frac{1}{2}\right) \, . \qquad (3.9)$$

If $\ell > 0$, we have $E_n = \hbar\omega_c(n + 1/2)$. On the other hand, if $\ell = -|\ell|$, then we have the same expression above with n changed by $n + |\ell|$, with n and $|\ell|$ being

non negative integers. From a theoretical point of view, the electrons on an interface as showed in figure 3.1 are confined by an infinite square well potential in the $z-$direction ($0 \leq z \leq d$). This way, we have $k_z = \frac{l\pi}{d}$, where $l = 1, 2, 3...$ Notice that, in contrast with either the flat sample or a sample with disclination, this transverse mode now contributes to Hall conductivity. In the Landau levels (3.6), the effective angular momentum is

$$\nu = \ell - \beta \frac{l\pi}{d} \; . \tag{3.10}$$
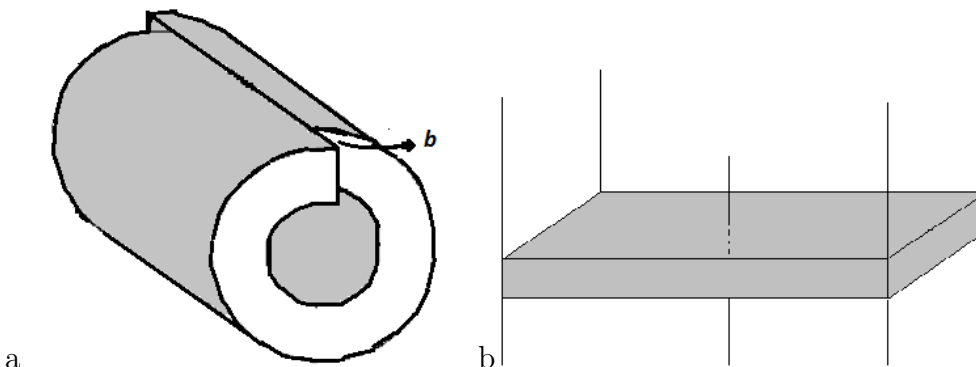

Figure 3.1: **a)** Cylindrical portion of a 3D solid showing the dislocation. **b)** Interface on a 3D solid with a screw dislocation. The line crossing the center of the figure represents the dislocation core.

In order to complete our analysis, we will consider a third type of defect called dispiration. It corresponds to a singular curvature and a singular torsion along the defect line. This defect is described by the following metric[30],

$$ds^2 = (dz + \beta d\phi)^2 + d\rho^2 + \alpha^2 \rho^2 d\phi^2 \; . \tag{3.11}$$

Notice that we have just the inclusion of the parameter α(the deficit/excess angle) in metric (3.1). Then, the parameter ν is now given by

$$\nu = \frac{\ell - \beta \frac{l\pi}{d}}{\alpha} \; . \tag{3.12}$$

If $\alpha = 1$, which means no curvature, we recover expression (3.10).

In what follows, we are interested in the physical consequences due to the presence of a screw dislocation on a 2DEG. We will consider the case $\alpha = 1$ first. The influence of α was investigated in reference [14] but we will show here how the Hall effect is influenced by the presence of both a disclination and a screw dislocation.

3.2 Hall Conductivity

In this section, we first compute the Hall conductivity on a 2DEG showing a screw dislocation characterized by the parameter β. As we have pointed out before, the

Hall conductivity is independent of a particular sample geometry. As in the previous chapter, we have

$$\sigma_H = -j\sigma_o \, , \tag{3.13}$$

Consider that only the fundamental state in the transverse direction is occupied. From the condition (3.8) , we have

$$-1 + \pi\frac{\beta}{d} < \ell < 1 + \pi\frac{\beta}{d} \, . \tag{3.14}$$

Taking into account only the case $\pi\frac{\beta}{d} < 1$, the possible values for the angular momentum are $\ell = 0, 1$. For each Landau level n, we have

$$E_{n,1} = \hbar\omega_c \left(n + \frac{1}{2} \right) \, , \tag{3.15}$$

for $\ell = 1$ and

$$E_{n,0} = \hbar\omega_c \left(n + \pi\frac{\beta}{d} + \frac{1}{2} \right) \, , \tag{3.16}$$

for $\ell = 0$.

From these two last equations, we can see how the degeneracy of the Landau Levels is broken, that is, each Landau level split in two other levels. In figure 3.2 we show how they are distributed.
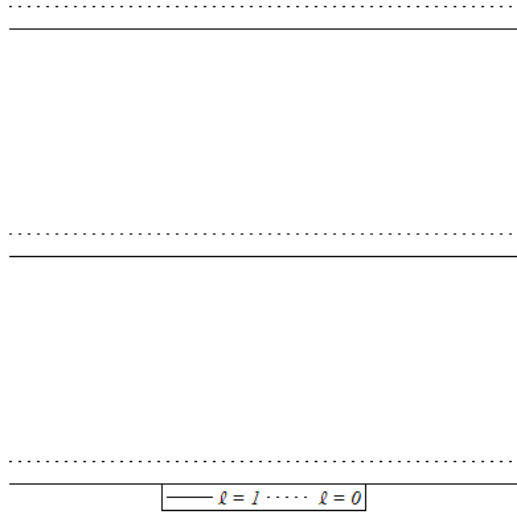
Figure 3.2: Landau Levels distribution for $\pi\frac{\beta}{d} < 1$. The solid lines are for $E_{n,1} = \hbar\omega_c \left(n + \frac{1}{2} \right)$ and the dotted lines are for $E_{n,0} = \hbar\omega_c \left(n + \pi\frac{\beta}{d} + \frac{1}{2} \right)$ (the energy spacing depends on the ratio $\pi\frac{\beta}{d}$).

In equations (3.15) and (3.16), we have $n = 0, 1, 2, 3...$ Performing the transformation $n = n_o - 1$, with $n_o = 1, 2, 3...$, equations (3.15) and (3.16) yield

$$n_o = \left[\frac{1}{4} + \frac{E_F}{2\hbar\omega_c} \right] \tag{3.17}$$

and

$$n_o^{'} = \left[-\frac{1}{4} - \frac{\pi\beta}{2d} + \frac{E_F}{2\hbar\omega_c} \right] , \tag{3.18}$$

respectively($[x]$ is the integer part of x). Suppose that, for some value of the external magnetic field, we have $E_{n,0} = E_F$(dot lines in fig.2), with $n = n_o - 1$. As we raise the magnetic field intensity, the next LL which will coincide with the Fermi energy is $E_{n,1}$, with $n = n_o - 1$(solid lines in fig.2). This situation corresponds to a Hall conductivity being diminished by one quantum σ_o. From equation $E_{n,1} = E_{n,0} = E_F$, we find the plateau width in this transition as

$$\Delta B = \frac{m^* E_F}{\hbar e} \frac{\frac{b}{2d}}{\left(n_o - 1/2 + \frac{b}{2d} \right) \left(n_o - 1/2 \right)} . \tag{3.19}$$

As we continue to raise the external magnetic field intensity, one quantum of conductivity σ_o is diminished again and we have transitions from $E_{n+1,\,1} = E_F$(solid lines in fig.2) to $E_{n,0} = E_F$(dot lines in fig.2). In this case, the plateau width is

$$\Delta B^{'} = \frac{m^* E_F}{\hbar e} \frac{1 - \frac{b}{2d}}{\left(n_o - 1/2 + \frac{b}{2d} \right) \left(n_o + 1/2 \right)} , \tag{3.20}$$

We have considered that $\beta = b/2\pi$. The two types of plateaus found above have lower widths in comparison to the flat case. Notice that if $b \equiv 0$, $\Delta B = 0$ and $\Delta B^{'}$ coincides with the plateau width for a flat sample without defects.

For a sample with a dispiration, the condition (3.8) yields

$$-\alpha + \pi\frac{\beta}{d} < \ell < \alpha + \pi\frac{\beta}{d} . \tag{3.21}$$

For a deficit angle($\alpha < 1$), the LL's are

$$E_{n,0;\alpha} = \frac{\hbar\omega_c}{\alpha} \left(n + \frac{b}{2d\alpha} + \frac{1}{2} \right) . \tag{3.22}$$

Notice that there is no energy splitting in this case since condition (3.8) allows $\ell = 0$ only. However, the energy spacing is affected and the plateau width is given by

$$\Delta B = \frac{\alpha m^* E_F}{\hbar e} \frac{1}{\left(n_o + \frac{b}{2d\alpha} \right)^2 - \frac{1}{4}} . \tag{3.23}$$

Without the screw dislocation ($b \equiv 0$), expression (3.23) will be the same as that found in reference [14] for a deficit angle α. In that reference, it was observed that the defict angle decreases the quantum Hall plateau widths, shifting the steps in the Hall conductivity to lower magnetic fields as wel as the Hall conductivity to lower values. The presence of a screw dislocation in this case changes only a plateau width for a specific value of deficit angle α. The screw dislocation diminishes the plateau width, shiffitng it even more to lower magnetic fields (see fig. 3.2).

In Figure 3.2 we plot the Hall conductivity for some values of the ratio b/d. We also plot σ_H in the case without screw dislocation, which we call *flat case*. All the

graphics start with the same filling factor at $B = 10T$. This happens because of the formula (3.17) which is the same as in the flat case. We can see that the steps on the Hall conductivity shift to lower magnetic fields but there is no shifting in the Hall conductivity.

As we raise the ratio b/d, the plateaus (3.19) get higher and the ones given by (3.20) diminish. On the other hand, as $b/d \to 0$, the influence of a screw dislocation as well as the thickness of the sample on the Hall conductivity approaches the Hall conductivity for a sample without defects. For an excess angle, the situation is quite
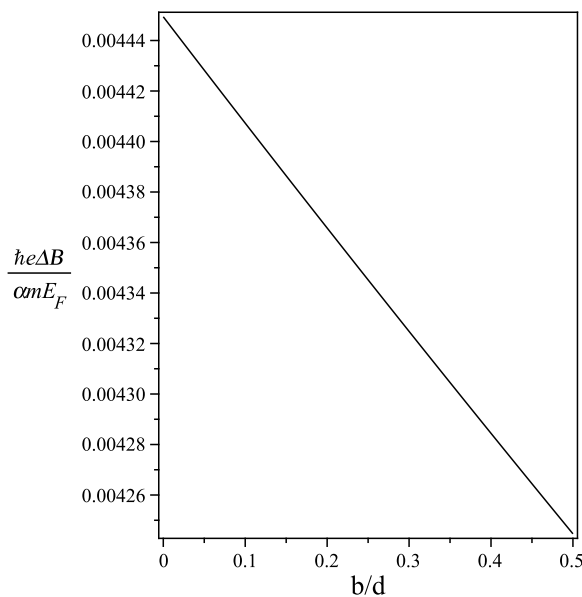

Figure 3.3: Plot of eq. (3.23) for a deficit angle $\alpha = 0.7$ and $n_o = 15$. The screw dislocation diminishes the plateau width, shiftting it to lower values. The Hall conductivity remains the same, that is, $\sigma_H = 15\sigma_o$. The same occurs at any n_o.

different. The condition (3.8) yields $\ell = -1, 0, 1$. This means that each LL with index n_o splits as

$$
\begin{aligned}
E_{n_o,1} &= \frac{\hbar\omega_c}{\alpha}\left(n_o - \frac{1}{2}\right) , \\
E_{n_o,0} &= \frac{\hbar\omega_c}{\alpha}\left(n_o + \frac{b}{2d\alpha} - \frac{1}{2}\right) , \\
E_{n_o,-1} &= \frac{\hbar\omega_c}{\alpha}\left(n_o + \frac{b}{2d\alpha} + \frac{1}{\alpha} - \frac{1}{2}\right) .
\end{aligned}
\tag{3.24}
$$

Their plot is depicted in Figure 3.2. Consider $E_F = E_{n_o,1}$. As we raise the magnetic field intensity, the next lower LL coinciding with E_F will be $E_{n_o-1,0}$. Continuing to raise the magnetic field, a transition goes from this level to $E_{n_o-1,-1}$ and the next
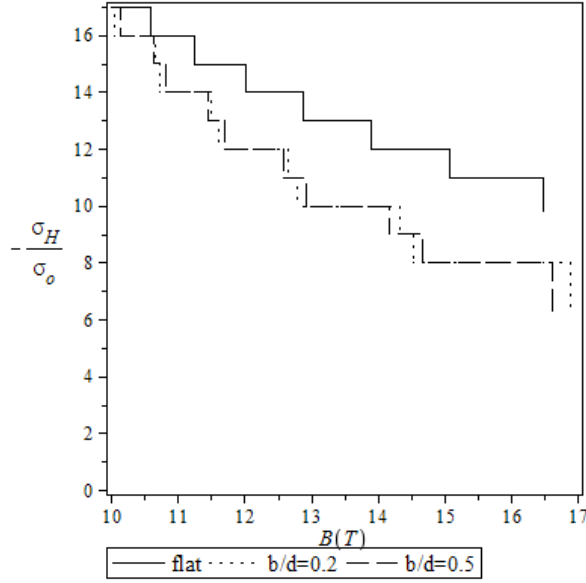
Figure 3.4: Hall conductivity versus magnetic field B for different values of the ratio b/d. The quantum Hall plateau widths decrease and the steps in the Hall conductivity are shifted to lower magnetic fields in comparison to the flat case($b/d \equiv 0$). Notice that there is no shifting in the Hall conductivity.

one goes from this level to $E_{n_o-1,1}$. We then get three different plateaus,

$$
\begin{aligned}
\Delta B_1 &= \frac{m^* E_F}{\hbar e} \frac{\alpha - 1 - \frac{b}{2d}}{\left(n_o + \frac{1}{\alpha} + \frac{b}{2d\alpha} - \frac{3}{2}\right)\left(n_o - \frac{1}{2}\right)} , \\
\Delta B_2 &= \frac{m^* E_F}{\hbar e} \frac{1}{\left(n_o + \frac{1}{\alpha} + \frac{b}{2d\alpha} - \frac{3}{2}\right)\left(n_o - \frac{3}{2} + \frac{b}{2d\alpha}\right)} , \\
\Delta B_3 &= \frac{m^* E_F}{\hbar e} \frac{\frac{b}{2d}}{\left(n_o - \frac{3}{2}\right)\left(n_o - \frac{3}{2} + \frac{b}{2d\alpha}\right)} .
\end{aligned}
\tag{3.25}
$$

In Figure 3.5, we see that the presence of an excess angle causes a shifting of the steps to higher magnetic fields and the Hall conductivity is shifted to higher values as well. Notice that at $10T$, the filling factor for a sample without a disclination is 17 while in the presence of it is 22. This plot was done considering equations (3.25). For a dispiration, there are three different expressions for the plateaus. If we consider the absence of screw dislocations, equations (3.25) will be given by $\Delta B_1 = \Delta B_2 \neq \Delta B_3$. That is, we have only two types of plateaus, as it was found in reference [14] where just the influence of disclinations was investigated. On the other hand, if we take $\alpha = 1$ in equations (3.25), we recover those expressions for a screw dislocation, (3.19) and (3.20).

31
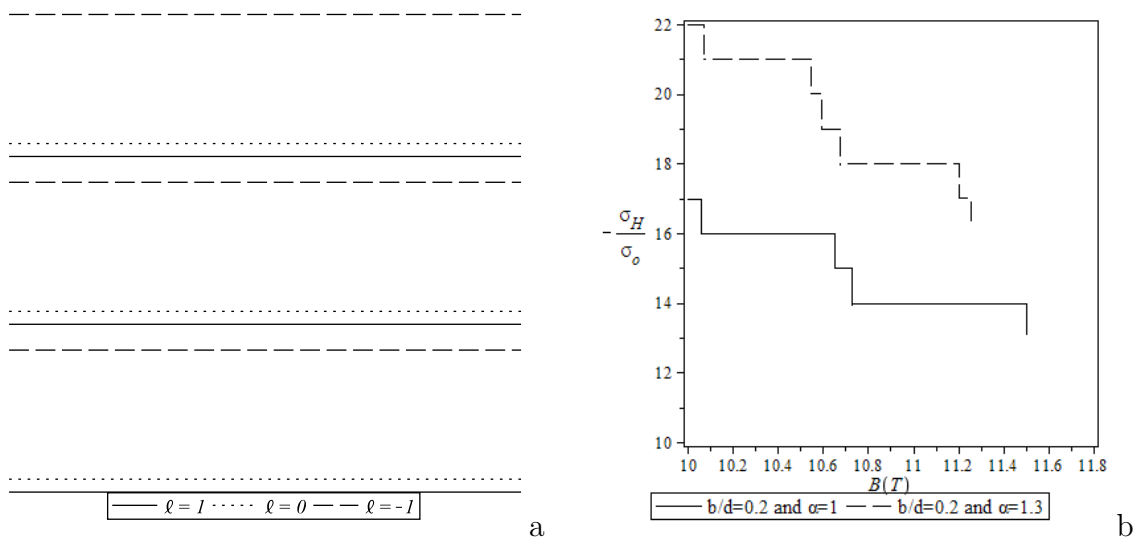
Figure 3.5: **a)** Landau levels on a sample showing a dispiration and **b)** Hall conductivity on a 2DEG with a screw dislocation(lower curve) and with a dispiration(upper curve). Notice that while the screw dislocation shifts only the plateaus to lower magnetic fields(see figure 4), the presence of a disclination with an excess angle α makes the Hall conductivity shift as well.

Conclusion

In this work we studied, for the first time, the integer quantum Hall effect on a cone. We have shown that considering the coupling between the wave functions and the singular scalar curvature (the conical tip), the profile of the Hall conductivity versus the external magnetic field modifies significantly.

On a first work, we have consider the range of coordinate l for the cone as $0 < l < +\infty$ and calculated the Shrodinger equation to obtain the Landau levels and finally obtain the values of Hall conductivity.

Then, for the cone without singularity at the tip, or with regular wave function, we have the appearance of infinite degeneracy lifting introduced by the angular momentum j, and for the cone with singularity, or irregular wave funtcion, we have just the split of the energy levels because of the plus and minus signs in its equation.

Because of this degeneracy lifting, we obtain an infinite number of small Hall conductivity plateaus for the case of the cone without singularity. The Hall conductivity then decreases rapidly in a smaller interval of magnetic field, than in the case of cone with singularity or the simple case.

By studying these two cases in more details, i.e. by varying some parameters such as the opening angle α of a cone, or removing the geometric potential given by the mean curvature, we have noticed that it is very easy to vary the Hall conductivity. In fact, the curvature reduces the range of the magnetic field that we need to obtain our plateaus.

We have also seen, by changing the opening angle α of the cone, that we have a shifting of the plateaus of the Hall conductivity.

To finish, we have considered two different models for electrons on a curved surface. One contains an effective scalar potential, proportional to the Gaussian curvature on the surface, while the other one shows an effective scalar potential which contains both the Gaussian and mean curvature on the surface. So, we have seen that the profile of the Hall conductivity shows discrepancies when we compare the two theories, depending on the opening angle of the cone.

In our work, if we consider the case without any singularity at the tip, we can extend our investigation to the double cone case, by taking the range of coordinate $-\infty < l < +\infty$.

On a second work, we have studied the effect of a screw dislocation on the Hall conductivity. It was shown that the thickness of the sample changes the position of the quantum Hall plateaus. We have shown that the torsion of the medium, β, decreases the quantum Hall plateau widths and shifts the steps in the Hall conductivity to lower values of magnetic fields. However, the Hall conductivity itself is not

shifted. We noticed the appearance of two types of plateaus in this case, like the case of the cone without singularity. This has happened because of the split of each Landau level in two other levels, for $\ell = 0, 1$.

In order to appreciate the presence of both, a screw dislocation and a disclination, we have considered a 2DEG with a dispiration. The steps in the Hall conductivity shift to lower values of magnetic fields when we have a deficit of angle($\alpha < 1$) [14]. The screw dislocation diminishes the plateau width for a specific value of a deficit of angle but does not shift the Hall conductivity. In the case of an excess angle($\alpha > 1$), the presence of a screw dislocation induces three different expressions for the plateaus since the Landau levels now splits for $\ell = -1, 0, 1$. In this case, there is a shift of the steps to higher magnetic fields.

In summary, the study carried out here can be realized in usual semiconductors. However, it shows important features if one has intention to deal with non planar 2DEG in other class of materials.

In this report, we have tried to take into account some geometric parameters to show how the inclusion of geometric factors is important and how the results can be different.

The theory based on the da Costa approach (with the presence of mean curvature) is a result of particle confinement and it is the same for electrons and holes. A similar confining procedure for relativistic carriers in graphene was first addressed in [33]. From the results we addressed here, we may note that the model one takes to investigate carries on to curved graphene is going to be relevant. Without the confinement procedure, which in our case led to the mean curvature contribution to the quantum Hall effect, the theory may not fit well the experiments on curved 2DEG. In the case of graphene cones[34], the conical geometry, which appears due to the presence of topological defects, must be investigated carefully since the singular Gaussian curvature may also affect the electronic transport in this material.

In performing this study, we hope to provide some answers about the behavior of the Hall conductivity in a particular geometry. We also hope that these theoretical bases can be reused for an experimental application.

Bibliography

[1] L. I. Magarill, A. V. Chaplik and M. V. Entin, Physics−Uspekhi **48** (9) 953 (2005)

[2] A. V. Chaplik, L. I. Magarill and D. A. Romanov, Physica B **249-251** 377 (1998).

A. B. Vorobe'v, K. J. Friedland, H. Kostial, R. Hey, U. Jahn, E. Wiebicke, J. S. Yukecheva, V. Y. Prinz, Phys. Rev. E **75**, 205309 (2007);

G. J. Meyer, N. L. Dias, R. H. Blick and I. Knezevic, IEEE Trans. on Nanotechnology **6** 446 (2007).

G. Ferrari, A. Bertoni, G. Goldoni and E. Molinari, Phys. Rev. E **78** 115326 (2008).

[3] C. L. Foden, M. L. Leadbeater and M. Pepper, Phys. Rev. B **52** R8646 (1995).

[4] D. V. Bulaev, V. A. Geyler and V. A. Margulis, Physica B **337** 180 (2003).

[5] D. V. Bulaev and V. A. Margulis, Eur. Phys. J. B **36** 183 (2003).

[6] D. V. Bulaev and V. A. Margulis, *Eur. Phys. J. B* **36**, (2003) 183 ;

A. Lorke , S. Böhm and W. Wegscheider, Superlattices and Microstructures **33**, (2003) 347;

L. I. Magarill , A. V. Chaplik and M. V. Entin, Physics-Uspekhi **48**, (2005) 953 ;

A. B. Vorobe'v , K. J. Friedland , H. Kostial , R. Hey, U. Jahn, E. Wiebicke , J. S. Yukecheva and V. Y. Prinz, *Phys. Rev. E* **75**, (2007) 205309 ;

A. Jellal, Nuclear Physics B **804**, [PM] (2008) 361;

K. J. Friedland, A. Siddiki, R. Hey, H. Kostial, A. Riedel, and D. K. Maude, Phys. Rev. B **79**, (2009) 125320;

C. Filgueiras and B. F. de Oliveira, Ann. of Phys.(Berlin) **523**, (2011) 898

[7] S. Mendach, O. Schumacher, Ch. Heyn, S. Schn. ull, H. Welsch and W. Hansen, Physica E **23**, (2004) 274.

[8] V.Ya. Prinz, V.A. Seleznev, A.K. Gutakovsky, A.V. Chehovskiy, V.V. Preobrazhenskii, M.A. Putyato and T.A. Gavrilova, Physica E **6**, (2000) 828;

V.Ya. Prinz, D. Grtzmacher, A. Beyer, C. David, B. Ketterer and E. Deccard, Proceedings of Ninth International Symposium on Nanostructures: Physics and Technology, St. Petersburg, Russia, 18-22 June, 2001, p. 13

[9] Y. N. Joglekar, A. Saxena, Phys. Rev. B **80** ,153405 (2009);

R. Dandoloff, A. Saxena, B. Jensen, Phys. Rev. A **81** , 014102 (2010);

R. Dandoloff, A. Saxena, B. Jensen, Phy. Rev. B **79**, 033404 (2009).

[10] M. O. Katanaev, Physics-Uspekhi **48** 675 (2005).

[11] C. Furtado , B. G. C. da Cunha, F. Moraes, E. R. B. de Mello and V.B. Bezerra, Phys. Lett. A **195**, (1994) 90

[12] C. Furtado and F. Moraes, Europhys. Lett. **45**, (1999) 279.

[13] C. Filgueiras, E. O. Silva, W. Oliveira, and F. Moraes, Ann. Phys. 325, (2010) 2529.

[14] A. A. de Lima and C. Filgueiras, Eur. Phys. J. B **85**, (2012) 401.

[15] C. Filgueiras and F. Moraes, Ann. of Phys. **323** (2008) 3150.

[16] B. Jensen, R. Dandoloff, Phys. Lett. A **375**, (2011) 448 .

[17] M. O. Goerbig, *Quantum Hall Effects*, arXiv:1998v2 (2009).

[18] M. P. do Carmo, *Differential Geometry of Curves and Surfaces* (Prentice Hall,1976).

[19] M.H. Al−Hashimi and U.−J. Wiese, Annals of Physics **323** (2008) 82.

[20] G. Ferrari, G. Cuoghi, Phys. Rev. Lett. **100** (2008) 230403 .

[21] R. C. T. da Costa, Phys. Rev. A **23** (1981) 1982 .

[22] K. Kowalski, J. Rembieliński, Ann. of Phys. **329** (2013) 146.

[23] M. Abramowitz and Irene A. Stegun, editors. *Handbook of Mathematical Functions.* New York: Dover Publications, 1972.

[24] M. Reed, B. Simon, in: Methods of modern mathematical physics; Functional analysis, vol. I, Academic Press, New York, London, 1972;

M. Reed, B. Simon, in: Methods of modern mathematical physics; Fourier analysis, self-adjointness, vol. II, Academic Press, New York, London, 1975.

[25] M. G. Alford, J. March-Russell and F.Wilczek, Nucl. Phys. B **328** (1989) 140 ;

Ph. de Sousa Gerbert, Phys. Rev. D **40** (1989) 1346;

P. de Souza Gerbert, R. Jackiw, Commun. Math. Phys. **124** (1989) 229;

B. S. Kay and U. M. Studer, Comm. Math. Phys. **139** (1991) 103 ;

D. K. Park and Jae Geub Oh, Phys. Rev. D **50** (1994) 7715 ;

G. Bonneau, J. Faraut, G. Valente, Am. J. Phys. **69** (2001) 322;

K. Kowalski, K. Podlaski, J. Rembieliński, Phys. Rev. A **66** (2002) 032118;

P. R. Giri, Phys. Rev. A **76** (2007) 012114;

F. M. Andrade, E. O. Silva and M. Pereira, Phys. Rev. D **85** (2012) 041701;

F. M. Andrade and E. O. Silva, Phys. Lett. B **719** (2013) 467.

[26] C. Filgueiras, E. O. Silva, W. Oliveira, and F. Moraes, Ann. Phys. **325** (2010) 2529.

[27] C. R. Hagen, D. K. Park, Ann. Phys. **251** (1996) 45;

C. R. Hagen, Phys. Rev. A **77** (2008) 036101.

[28] M. O. Goerbig, *Quantum Hall Effects*, arxiv:0909.1998v2.

[29] M. G. Alford, J. M. Russell and F. Wilczek, Nucl. Phys. B **328**, (1989) 140;

P. S. Gerbert, Phys. Rev. D **40**, (1989) 1346;

P. S. Gerbert and R. Jackiw, Commun. Math. Phys **124**, (1989) 229;

C. R. Hagen, Phys. Rev. Lett **64**, (1990) 503;

C. R. Hagen, Phys. Rev. D **42**, (1993) 5935;

C. R. Hagen and D. K. Park 1996 *Ann. Phys. (NY)* **251** 45;

K. Kowalski , K. Podlaski and J. Rembieliński, Phys. Rev. A **66**, (2002) 032118;

C. Filgueiras and F. Moraes, Phys. Lett. A **361**, (2007) 13;

C. Filgueiras and F. Moraes, Ann. of Phys. (N.Y.) **323**, (2008) 3150;

F. M. Andrade, E. O. Silva and M. Pereira, Phys. Rev. D **85**, (2012) 041701;

C. Filgueiras, F. M. Andrade and E. O. Silva, J. Math. Phys. **53**, 122106 (2012);

F.M. Andrade and E.O. Silva, Phys. Lett. B **719** (2013) 467.

[30] G. de A. Marques, C. Furtado, V. B. Bezerra and F. Moraes, J. Phys. A: Math. Gen. **34**, (2001) 5945.

[31] R. C. T. da Costa, Phys. Rev. A **23**, 1982 (1981).

[32] C. Filgueiras, E. O. Silva, F. M. Andrade, J. Math. Phys. **53**, 122106 (2012).

[33] V. Atanasov, A. Saxena, Phys. Rev. B **81**, 205409 (2010).

[34] P. E. Lammert and V. H. Crespi, Phys. Rev. B **69**, 035406 (2004).

[35] A. L. Silva Netto and C. Furtado, J. Phys.: Condens. Matter, 20 125209 (2008).

Appendix A

Quantum mechanics on curved surfaces

In the two-dimensional case, it is interesting for us to study the curvature effects, for example the curvature effects on the conductance and on the magnetization. Actually, we have explained the flat case. But it is more interesting to investigate in Non-Planar 2-Dimensional Electron Gas (NP2DEG). Obviously, when we study a curved surface, that introduces new parameters to be taken into account.
Effectively, for the case of a curved surface, we can used several kinds of approaches. Let us consider both of them on a conic surface. In the first one, we consider that the charge carries are bound to the surface by a constraining potential, and not in the second approach. Let us briefly describe their general ideas.

A.1   The da Costa approach

The first approach is based on the da Costa's theory, published in 1981. This theory is applied to a surface with such a small thickness that we consider $d \to 0$. The general idea on this theory it is deriving the Schrödinger equation of a free particle constrained to move on a curved surface [31], starting from the 3D and then reducing it to a 2D equation by a confining procedure. This constraint is an external potential limiting the motion of non-interacting electrons to a thin interface, with constant thickness. Then we get the following Schrödinger equation [32]

$$-\frac{\hbar^2}{2m}\frac{\partial^2 \chi_n}{\partial q_n^2} + V(q_n)\chi_n = E_n\chi_n, \tag{A.1}$$

with q_n the normal coordinate, and $V(q_n)$ the potential that confines the particle to the thin interface. In the coordinates of a curved surface, we have

$$\frac{1}{2m}\left[-\frac{\hbar^2}{\sqrt{g}}\partial_\mu \left(\sqrt{g}g^{\mu\nu}\partial_\nu \right) \right]\Psi + V_{DC}\Psi = E_n\Psi, \tag{A.2}$$

where $g^{\mu\nu}$ is the contravariant component of the metric tensor, $g = \det g_{\mu\nu}$, and V_{DC} the scalar geometric potential, whose expression is

$$V_{DC} = -\frac{\hbar^2}{2m}\left(H^2 - K\right),\tag{A.3}$$

where $H = \frac{(\kappa_1 + \kappa_2)}{2}$ it is the mean curvature, and $K = \kappa_1 \kappa_2$ is the Gaussian curvature of the surface, while κ_1 and κ_2 are the principal curvatures of the surface.

A.2 The Dirac approach

Now, if we take the intrinsic second order Dirac theory, for a 3-dimensional space, based on the Klein-Gordon equation, without the constraining potential, like the following equation

$$-\frac{\hbar^2}{2m}\nabla_{\parallel}^2 \psi + \frac{\hbar^2}{4m}R\psi = E_c \psi,\tag{A.4}$$

with $\nabla_{\parallel}$ is the usual covariant derivative acting on a scalar function, ψ a definite spin-state, $E_c = E - m$ the classical energy mesure and R the Ricci curvature scalar in the static surface. We confined in 2D, with $R = 2K$, where K is the Gaussian curvature of a surface. So, we obtain the effective potential

$$V_{KG} = \frac{\hbar^2}{2m}K,\tag{A.5}$$

We obtain an expression for the geometric potential different from the first case. But for both, we have

$$H = \frac{1}{2}\frac{eG - 2fE + gE}{EG - F^2}\tag{A.6}$$

and

$$K = \frac{1}{2}\frac{eg - f^2}{EG - F^2},\tag{A.7}$$

knowing that (E, F, G) and (e, f, g) are respectively the coefficients of the first fundamental form $(I = E \cdot du_1^2 + 2F \cdot du_1 du_2 + G \cdot du_2^2)$ and the second fundamental form $(II = e \cdot du_1^2 + 2f \cdot du_1 du_2 + g \cdot du_2^2)$ [18].

The biggest difference between V_{DC} and V_{KG} is that the first one is only attractive and the second can be attractive or repulsive [32]. But with this example briefly described, we can see that taking into account or not the geometric potential can change our results, because calculating geometric potential allows us to say that we are in a curved geometry, and not on a planar geometry.

In this examples, we have considered just the case for the free electrons. Into the scope of this study, if we consider the electrons in the presence of magnetic field, we have to operate the change : $\partial_\mu \longrightarrow \partial_\mu - eA_\mu$.

Appendix B

Details of calculation of the Schrödinger equation for a cone

We have seen in the section 1.3 that the Hamiltonian for a charged particle is

$$\hat{H} = \frac{1}{2m}(\mathbf{p} - e\mathbf{A})^2. \tag{B.1}$$

Or we know that $\mathbf{p} = (p_l, p_\varphi, p_z)$ and $\mathbf{A} = (0, \frac{B_z l sin\varphi}{2}, 0)$, so if we develop our equation, we get

$$\hat{H} = \frac{\hat{p_l}^2}{2m} + \frac{1}{2m}(\hat{p_\varphi} - e\hat{A}_\varphi)^2. \tag{B.2}$$

By using $p_l^2 = -\hbar^2 \nabla_l^2$, with $\nabla_l^2 \equiv \frac{1}{\sqrt{g}}\partial_l \sqrt{g} g^{11}\partial_l$, $g = det(g_{ij}) = l^2 \sin^2\alpha$, where g_{ij} is the metric tensor, and $p_\varphi = -\frac{i\hbar}{l\sin\alpha}\partial_\varphi$, we obtain

$$\hat{H} = -\frac{\hbar^2}{2m}\frac{1}{l}\frac{\partial}{\partial l}\left(l\frac{\partial}{\partial l}\right) - \frac{1}{2m}\left(-\frac{i\hbar}{l\sin\alpha}\frac{\partial}{\partial\varphi} - \frac{eB_z l \sin\alpha}{2}\right)^2. \tag{B.3}$$

But in order to ensure the hermiticity of radial momentum operator, $\hat{p}_l$, it must act on the radial wave functions as

$$\hat{p}_l\psi(l) = -i\hbar\left(\frac{\partial}{\partial l} + \frac{1}{2l}\right)\psi(l). \tag{B.4}$$

For more details, see [19].
Finally we obtain the Schrödinger equation

$$\hat{H} = -\frac{\hbar^2}{2m}\left[\frac{1}{l}\frac{\partial}{\partial l}\left(l\frac{\partial}{\partial l}\right) - \frac{1}{4l^2} - \left(-\frac{i}{l\sin\alpha}\frac{\partial}{\partial\varphi} - \frac{e\sin\alpha B_z l}{2\hbar}\right)^2\right]. \tag{B.5}$$

Appendix C

Calculation for the geometric potential V_S

Let us now consider the geometric potential $V_s = -\frac{\hbar^2}{2m}(H^2 - K)$, where H and K are respectively the mean curvature and the Gaussian curvature. First, we need to calculate the first fundamental form [18] :

$$I = E \cdot du_1^2 + 2F \cdot du_1 du_2 + G \cdot du_2^2 \tag{C.1}$$

To know the coefficients E, F and G, we have to use the metric tensor $E = g_{11} = 1$, $F = g_{12} = 0$ and $G = g_{22} = l^2 \sin^2(\alpha)$, so :

$$I = dl^2 + l^2 sin^2(\alpha) \cdot d\varphi^2 \tag{C.2}$$

Now, we get the second fundamental form :

$$II = e \cdot du_1^2 + 2f \cdot du_1 du_2 + g \cdot du_2^2 \tag{C.3}$$

with $e = \vec{n} \cdot \vec{X}_{\varphi\varphi} = \frac{\partial^2 \vec{X}}{\partial \varphi^2} = -l \sin(\alpha) \cos(\alpha)$, $f = \vec{n} \cdot \vec{X}_{\varphi l} = \frac{\partial^2 \vec{X}}{\partial \varphi \partial l} = 0$ and $g = \vec{n} \cdot \vec{X}_{ll} = \frac{\partial^2 \vec{X}}{\partial l^2} = 0$.

$$II = -l \sin(\alpha) \cos(\alpha) \cdot d\varphi^2 \tag{C.4}$$

Let us calculate the Gaussian curvature :

$$K = det(II) = \frac{eg - f^2}{EG - F^2} = 0 \tag{C.5}$$

and the mean curvature :

$$H = \frac{1}{2} tr(II) = \frac{1}{2} \frac{eG - 2fE + gE}{EG - F^2} = -\frac{\cos(\alpha)}{2l \sin(\alpha)} \tag{C.6}$$

So the geometric potential is :

$$V_s = \frac{-\hbar^2}{8m} \frac{\cos^2(\alpha)}{l^2 \sin^2(\alpha)} = \frac{-\hbar^2}{8m} \frac{(1 - \sin^2(\alpha))}{l^2 \sin^2(\alpha)}. \tag{C.7}$$

Appendix D

Kummer's function

To resolve this kind of Schrödinger equation (2.18), we take into account a confluent hypergeometric function, more precisely the generalized hypergeometric series M

$$M(a, b, z) = 1 + \frac{az}{b} + \frac{(a)_2 z^2}{(b)_2 2!} + ... + \frac{(a)_n z^n}{(b)_n n!} + ... \tag{D.1}$$

If we consider just the first order, or $(a)_0 = 1$, we obtain $M(a, b, z) = 1$.
The Tricomi confluent hypergeometric function $U(a, b, z)$ introduced by Francesco Tricomi (1947). The function U is defined in terms of Kummer's function M by

$$U(a, b, z) = \frac{\pi}{\sin(\pi b)} \left(\frac{M(a, b, z)}{\Gamma(1 + a - b)\Gamma(b)} - Z^{1-b} \frac{M(1 + a - b, 2 - b, z)}{\Gamma(a)\Gamma(2 - b)} \right) \tag{D.2}$$

By combining with the equation (D.2), we obtain for the variable (a, b, z), the values

$$\begin{cases} a = \frac{s}{2} + \frac{1}{4} - \frac{E}{2\omega} \\ b = s + \frac{1}{2} \\ z = m\omega l^2 = \gamma l^2 \end{cases}, \tag{D.3}$$

and we consider $C = \frac{\pi}{\sin(\pi b)}$.
We finally have

$$U(a, b, z) = C l^{-s} \left(\frac{l^s}{\Gamma(1 + a - b)\Gamma(s + \frac{1}{2})} - \frac{\gamma^{\frac{1}{2} - s} l^{-s+1})}{\Gamma(a)\Gamma(\frac{3}{2} - s)} \right). \tag{D.4}$$

This series, in order to have normalization of the wave function, must be a polynomial of degree n, where n is an integer, we obtain for each case $a = -n$, or

$$\frac{s}{2} + \frac{1}{4} - \frac{E}{2\omega} = -n, \tag{D.5}$$

like explained in [35].
So, we have $\Gamma(a) = \infty$, and the second part of our equation (D.4) is null. We have

$$U(a, b, z) = C \frac{1}{\Gamma(1 + a - b)\Gamma(s + \frac{1}{2})}. \tag{D.6}$$

We obtain a convergent function for each value of s.